

The magnetism of single-crystal αTmH_x solid solutions ($0 \leq x \leq 0.1$)

This article has been downloaded from IOPscience. Please scroll down to see the full text article.

1990 J. Phys.: Condens. Matter 2 7897

(<http://iopscience.iop.org/0953-8984/2/39/004>)

View [the table of contents for this issue](#), or go to the [journal homepage](#) for more

Download details:

IP Address: 171.66.16.151

The article was downloaded on 11/05/2010 at 06:54

Please note that [terms and conditions apply](#).

The magnetism of single-crystal α -TmH_x solid solutions ($0 \leq x \leq 0.1$)

J N Daou[†], J P Burger[†], P Vajda[†], G Chouteau[‡] and R Tur[‡]

[†] Hydrogène dans les Métaux (Unité associée au CNRS 803), Bâtiment 350, Université Paris-Sud, F-91405 Orsay, France

[‡] Service National des Champs Intenses, CNRS, F-38402 Grenoble, France

Received 28 March 1990

Abstract. The hydrogen concentration x of α -TmH_x solid solutions causes the anti-ferromagnetic transition temperature T_N and the ferrimagnetic transition temperature T_c (along the c axis), as well as the critical field necessary for the transformation into the ferromagnetic state, to decrease markedly. It appears also that T_N is very sensitive to the applied field H along c . The tendency of hydrogen to cause the ferrimagnetic and ferromagnetic magnetisation to decrease at low temperatures suggests that the hydrogen exerts an influence on the domain walls and the coercivity. The basal plane magnetisation, for which anisotropy also occurs, is favoured by hydrogen, and its temperature variation seems to show two types of transition at high fields.

1. Introduction

The magnetism of the heavy rare earths with hexagonal structure (Gd, Tb, Dy, Ho, Er and Tm) depends essentially on two energy terms [1].

(i) The first is the long-range RKKY spin–spin interaction energy

$$E = -\sum_{ij} J(R_{ij})S_i S_j \quad (1)$$

$$J(R_{ij}) \approx N(\varepsilon_F)\Gamma^2 F(2k_F R_{ij})$$

where Γ is the exchange integral between conduction electron spins s and localised spins S , $N(\varepsilon_F)$ is the Fermi level density of states, and $F(2k_F R_{ij})$ is the well known RKKY oscillating function. It leads to a magnetic transition, generally of antiferromagnetic (AF) type with a wavevector Q (helical ordering in the basal plane at T_H , or sinusoidal ordering along the c axis at T_N) with

$$T_H \approx T_N \approx N(\varepsilon_F)J(Q)S(S+1) \quad (2)$$

where $J(Q)$ is the Fourier transform of $J(R_{ij})$.

(ii) The second is the magnetic anisotropy energy of the form

$$E_A = -K(M^z)^2 + K'(M^z)^4 \quad (3)$$

where M^z (or M_Q^z) is the magnetisation along the c axis. The signs of K and K' determine the occurrence of the magnetisation ordering in the basal plane (for Gd, Tb, Dy and

Ho) or along the c axis (for Er and Tm). At lower temperatures, one observes often a further transition (from antiferromagnetism to ferromagnetism) whose origin can be related to magnetoelastic effects [1].

For pure Er, for example, one observes in fact three transitions: T_N along c , T_H in the basal plane and T_c along c . The first two transitions arise because $K > 0$ (which favours the c axis) and $K' > 0$ (which favours the basal plane). However, for Tm, the rare earth in the present study, there is only an AF transition along c , followed by a ferrimagnetic transition at T_c (or T_{\min}) $< T_N$. This new transition, for which it is difficult to define the temperature at which it occurs (T_{\min} corresponds to the minimum of the magnetisation below T_N , while T_c corresponds to the maximum of the slope dM/dT at temperatures below T_{\min}) results from a squaring of the incommensurate sinusoidal modulation (of wavevector Q) with occurrence of a commensurate seven-layer antiphase ferrimagnetism (four layers with spin up and three layers with spin down denoted 4–3). All this has been studied by neutron diffraction [2–4] and magnetisation measurements [5]. Although there is no magnetic ordering in the x – y basal plane (probably because $K' < 0$) the measured M^{xy} in an applied field H^{xy} along the a or b axis shows a well defined maximum at T_N , a fact which can be explained through an entropic coupling between M^{xy} and M_Q^z [6] such that

$$M^{xy} \approx H^{xy} / (T + C^{xy,z} (M_Q^z)^2). \quad (4)$$

The occurrence of the AF order parameter M_Q^z gives rise to an anomaly for M^{xy} at T_N , but it is a well defined maximum only if $K' < 0$.

An interesting feature, which we shall study in this work, concerns the effect of solid solution of hydrogen, i.e. α -TmH $_x$ compounds, with $x \leq 0.1$. The concentration x can affect the electronic structure (with a decrease in the number of conduction electrons), but also the anisotropy energy (through for instance modifications of the crystal field) as well as the magnetoelastic energy (because of the local expansion induced by the hydrogen atoms). TmH $_x$ polycrystals have been studied in the magnetic range by electrical resistivity [7], magnetisation [8, 9], neutron diffraction [10] and specific heat measurements [11]. For single crystals, magnetisation measurements have been done only on α -ErH $_x$ [12], while resistivity data exist for α -ErH $_x$ [13] and α -TmH $_x$ [14]. In the present work, we report on the strong effects of hydrogen on the magnetisation of single-crystal TmH $_x$, with applied fields parallel to the c axis or to the a and b axes in the x – y basal plane. Some new results for pure Tm will also be described.

2. Experimental procedure

A 1.3 mm \times 1.7 mm \times 4 mm sample was cut along the a , b , c axes of a thulium single crystal grown by the Ames Laboratories (Ames, IA, USA). After it had been first investigated in the pure state, it was then loaded successively with hydrogen at 500 °C to obtain the following concentrations x : 0.02, 0.05 and 0.1 atoms H/atoms Tm. The magnetisation measurements were done with a vibrating-coil magnetometer; the applied fields were in the range $50 \text{ G} \leq H \leq 50 \text{ kG}$ in the temperature interval $1.5 \text{ K} \leq T \leq 100 \text{ K}$. Demagnetisation corrections to the true internal field have been calculated when needed.

3. Results and discussion

3.1. Pure Tm ($x = 0$)

3.1.1. Magnetisation along the c axis. In figure 1 we give first some classical results [5] for the fields $H = 10 \text{ kG}$ and $H = 36 \text{ kG}$. For the former field, we observe the Néel

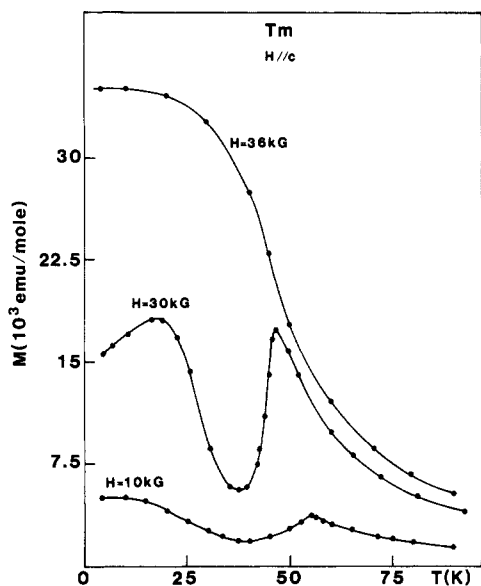


Figure 1. Temperature variation in the magnetisation M for pure Tm with fields applied parallel to the c axis.

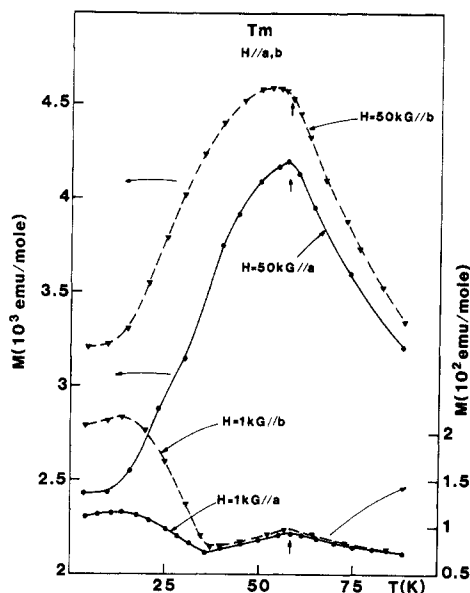


Figure 2. Temperature variation in the magnetisation M for pure Tm with applied fields parallel to the a and the b axes in the basal plane.

temperature T_N at 56 K, while for $T \leq T_{\min}$ (temperature of the minimum) the magnetisation increases up to a saturation value of 5×10^3 emu mol⁻¹, which corresponds nearly exactly to $1 \mu_B$, in good agreement with the 4–3 seven-layer ferrimagnetism. For the latter field, T_N disappears, i.e. the AF state (and the ferrimagnetic state) are transformed into a ferromagnetic state; the magnetisation M^z increases continuously with decreasing T and saturates at $T \approx 0$ towards $M \approx 7 \mu_B$, which corresponds to the theoretical value. However, a new result is obtained for an intermediate field $H = 30$ kG: T_N is still present (but at 47 K) while, at lower temperatures, M increases strongly beyond $1 \mu_B$ (up to about $3.5 \mu_B$), with a small decrease at lower temperatures ($T < 17$ K). This very surprising result could be because the critical field H_{cr} for the AF (or ferrimagnetic) \rightarrow ferromagnetic transition has a curious temperature dependence; we shall show later (figure 7) that H_{cr} increases first (near T_N) when lowering T and then decreases but increases again at still lower temperatures. This may lead to complicated competition between the AF and the ferromagnetic states.

3.1.2. Magnetisation along the a and b axes in the basal plane. At low fields, i.e. $H \approx 1$ kG (figure 2), M^a and M^b follow qualitatively M^z ; there is a well defined maximum at T_N (in agreement with equation (4)) and an increase for $T < T_{\min}$. This small increase arises probably because H^{xy} transfers a fraction of M^z , i.e. the ferrimagnetic component, into the x - y plane, through competition of the $-\mathbf{M} \cdot \mathbf{H}$ term with the anisotropy term (which favours the c axis).

At higher fields ($H \approx 50$ kG), the increase at low T disappears (no minimum observed), but the absolute value of M^{xy} is relatively large, about half of the ferrimagnetic M^z . The disappearance of the expected increase may then be because the contribution of $M^{xy}(H)$ from equation (4) is much larger than that from the ferrimagnetic magnetisation $M^z(H^z = 0)$. One can note also that for this large field there is a slight shift of the

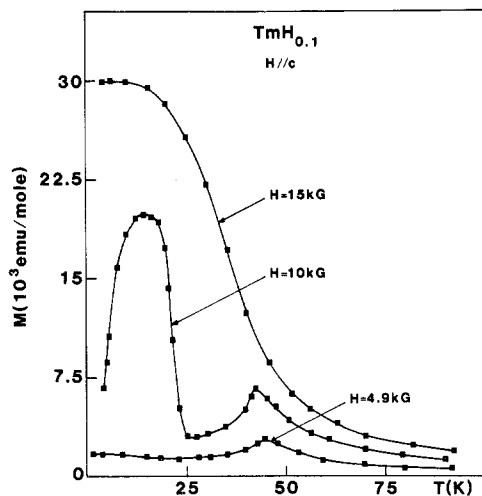


Figure 3. Temperature variation in the magnetisation for $\text{TmH}_{0.1}$ with applied fields parallel to the c axis.

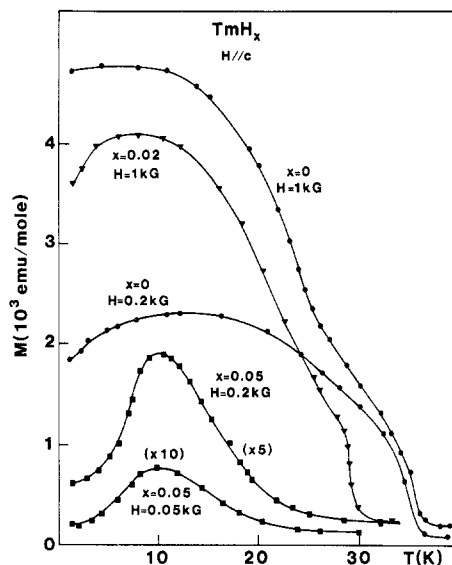


Figure 4. Low-temperature variation in the ferrimagnetic magnetisation for different low fields parallel to the c axis and for different hydrogen concentrations x .

maximum (especially for the b axis) compared with the value of T_N (indicated by the arrow), a fact which will be more visible for finite x -values.

3.2. TmH_x : effects of hydrogen

3.2.1. Properties along the c axis. Figure 3, for $x = 0.1$, is qualitatively similar to figure 1. For $H = 5$ kG, there is a well defined maximum of the magnetisation at $T_N = 45$ K, a value smaller than for $x = 0$, in agreement with earlier results [7–11]. The antiferromagnetism transforms into ferromagnetism for a field $H = 15$ kG, a value which is much smaller than for $x = 0$. It should also be noted that the saturation at low T is slightly smaller than for $x = 0$, which indicates perhaps that the anisotropy favouring the c axis has slightly decreased. For $H = 10$ kG, we observe an intermediate situation: the well defined AF maximum is followed by a sharp increase in M at low temperatures, an increase which is again much larger than that corresponding to the ferrimagnetic 4–3 transition. However, M drops steeply below 15 K which raises the following question: is this due to a return towards the 4–3 ferrimagnetic situation or is it due to magnetic domain effects with a pinning of the corresponding Bloch walls, favoured by the local atomic disorder and elastic distortion due to the H atoms?

As concerns the true ferrimagnetic transition (in lower fields), we give some results on figures 4 and 5. For $x = 0$, the saturation for a field $H = 1$ kG corresponds to the theoretical value $M = 1\mu_B$, while it is much smaller for $H = 0.2$ kG, a normal situation. However, for $x > 0$, the magnetisation of the 4–3 transition appears to be smaller than for $x = 0$ for equivalent fields H . A further difference arises because M tends to decrease again strongly below 10 K. In order to check whether the true 4–3 transition is still present, we have measured the saturation of M up to $H \approx H_{cr}$, the critical field for the destruction of the AF and ferrimagnetic states. Up to $x = 0.05$ we obtain nearly exactly

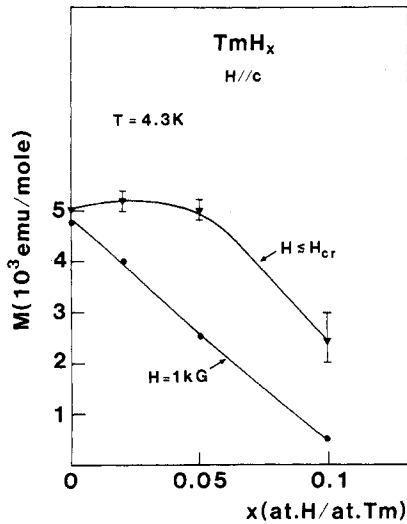


Figure 5. Hydrogen concentration dependence of the ferrimagnetic low-temperature magnetisation parallel to the c axis at constant field ($H = 1$ kG) or at the approach of the critical field H_{cr} .

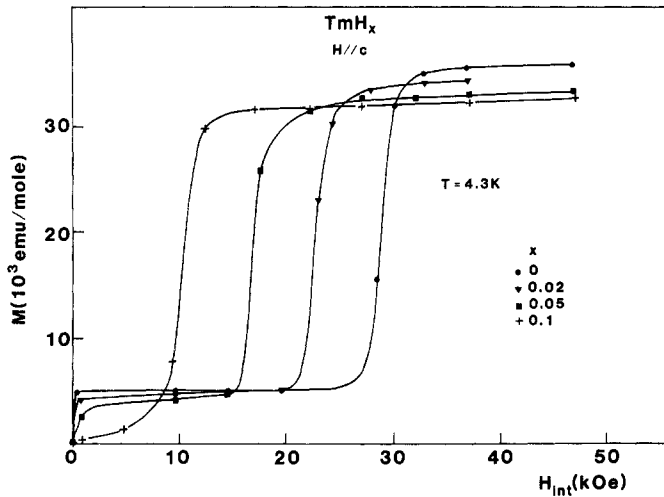


Figure 6. Field-induced ferrimagnetic-to-ferromagnetic transition parallel to the c axis at $T = 4.3$ K.

the theoretical 4–3 saturation value (figure 5), but not for $x = 0.1$, probably because the necessary field for the ferrimagnetic saturation is larger than the critical field H_{cr} establishing the complete ferromagnetism. This difficult saturation behaviour for $x > 0$ indicates again that the H atoms increase the coercivity fields, i.e. the hydrogenated samples are magnetically harder.

3.2.2. *Critical fields H_{cr} along the c axis.* Figure 6 shows that there are sharp field-dependent ferrimagnetic-to-ferromagnetic transitions at 4.3 K. The magnetisation M increases from the 4–3 value ($M = 1\mu_B$) to complete saturation ($M = 7\mu_B$ for $x = 0$). One observes, however, a slight decrease in this saturation value with x , which can be related as we mentioned before to a modification with x of the anisotropy terms K and

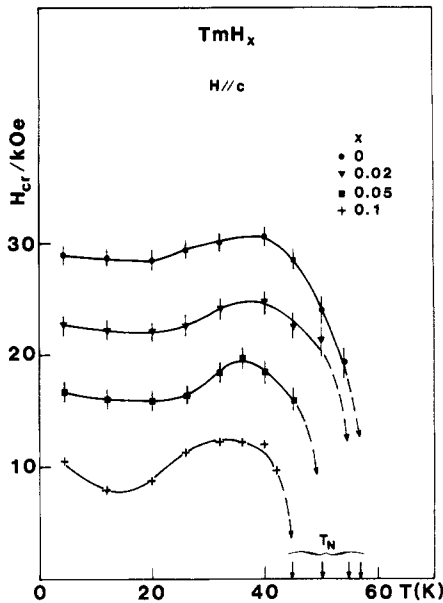


Figure 7. Temperature variation in the critical field H_{cr} parallel to the c axis for the AF (or ferrimagnetic)-to-ferromagnetic transition.

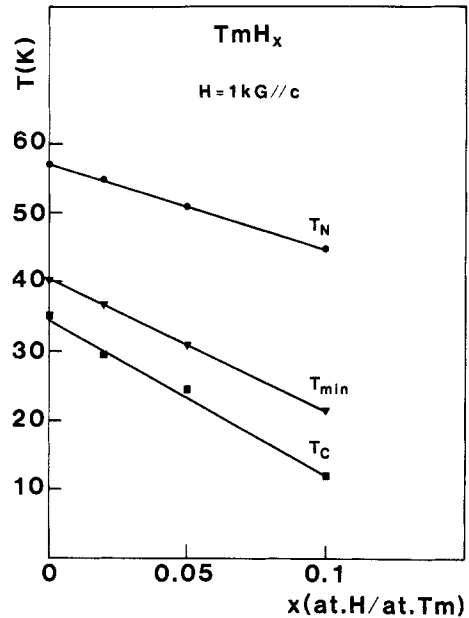


Figure 8. Variation with hydrogen concentration in the AF transition temperature T_N and the ferrimagnetic transition temperature T_c or T_{min} in a field $H = 1$ kG parallel to the c axis.

K' . In figure 7, one notes first that H_{cr} decreases strongly with increasing x , a fact related of course to the corresponding decrease in T_N with increasing x . Investigating this in detail, one finds that the temperature dependence of $H_{cr}(T)$ has a rather complicated behaviour: H_{cr} decreases first slightly with increasing T and then goes through a minimum followed by a maximum with a strong decrease when T tends towards T_N . The low-temperature behaviour of $H_{cr}(T)$ is completely different from that for ErH_x [12] where H_{cr} tended towards zero at $T = T_c$, the zero-field AF-to-ferromagnetic transition. Such a transition does not exist for TmH_x so that H_{cr} has a finite value at $T \approx 0$; the initial small decrease in H_{cr} with increasing T (accelerated by hydrogen) is probably related to the decrease in the energy difference between the ferrimagnetic and AF states.

3.2.3. Critical temperatures. In figure 8 we give the variation with x of the AF (T_N) and ferrimagnetic transition temperatures; for the latter, we characterise by T_{min} the temperature for which M goes through a minimum below T_N and by T_c the temperature for which dM/dT is a maximum below T_{min} . All these transition temperatures decrease with increasing x , which is identical with the $T_N(x)$ variation for ErH_x but opposite to the variation in the ferromagnetic $T_c(x)$ for ErH_x [12], indicating that the ferrimagnetic transition (for TmH_x) probably has a different origin from the ferromagnetic transition (for ErH_x). The decrease on the transition temperatures can be interpreted in terms of modifications of the electronic structure by x ; it is well known that hydrogen tends to cause the density of conduction electrons [13] and also the Fermi level density of states to decrease (by formation of low-energy metal-hydrogen bonding bands), leading to a decrease in T_N (equation (2)). Apparently, the ferrimagnetic transition (T_c, T_{min}) involves only modifications of $J(Q)$ by taking into account Fourier components (at $3Q$,

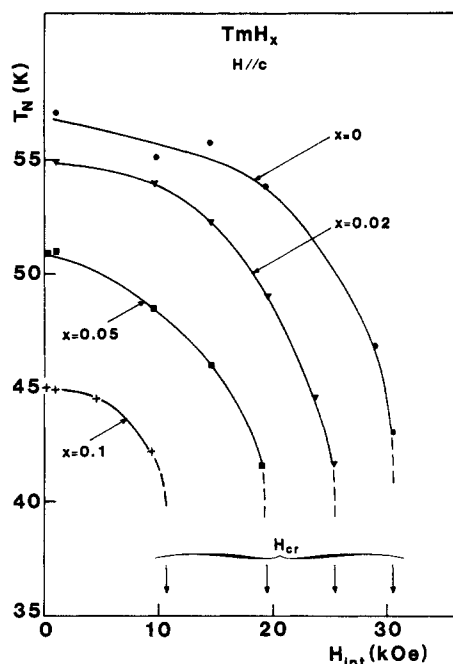


Figure 9. Field dependence (parallel to the c axis) of the AF transition temperature $T_N(x)$.

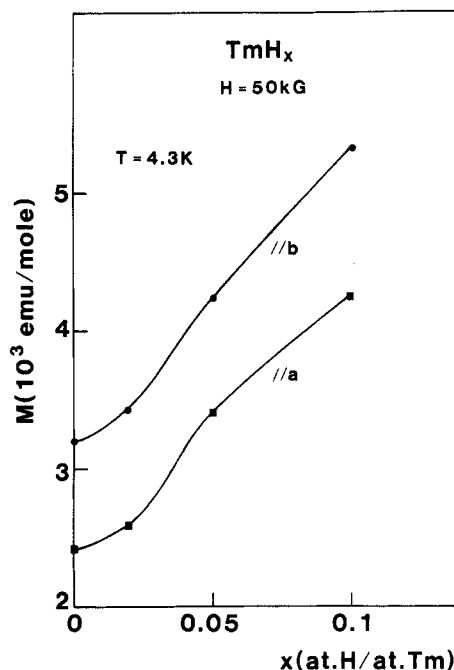


Figure 10. Variation with hydrogen concentration x in the basal plane magnetisation measured at 4.3 K with a field $H = 50$ kG parallel to the a and b axes.

$5Q, \dots$); the incommensurate sinusoidal modulation of S^z can thus square up into a commensurate ferrimagnetic state with four spin-up and three spin-down layers. If this is the case, then one can expect that the variation in $T_c(x)$ or $T_{\min}(x)$ is very similar to that of $T_N(x)$. One may of course ask why for TmH_x there is no true zero-field ferromagnetic transition as in ErH_x , for which this transition is related to magnetoelastic effects confirmed by the observed modifications of the lattice parameters a, b, c across T_c [16]. The corresponding coupling between magnetisation and the elastic strains [17] gives rise to an energy gain $-\Delta E_{\text{ME}}$ which leads to a ferromagnetic transition if $-\Delta E_{\text{ME}} < E(\text{AF}) - E(\text{ferro})$, the negative but purely magnetic energy difference, proportional to $J(Q) - J(0)$, with $J(Q) > J(0)$, between the AF and the ferromagnetic states. Apparently, this condition is not realised for Tm and TmH_x , a further argument being related to the fact that $T_c(x)$ increases with increasing x for ErH_x (possibly owing to the expansion induced by hydrogen), while $T_c(x)$ or $T_{\min}(x)$ decreases with increasing x for TmH_x .

In figure 9 we plot $T_N(x, H)$ as a function of the applied field H (parallel to c). One observes a strong decrease in T_N with increasing H , which is obviously due to the destabilising action of a static field on the antiferromagnetism. A qualitative Ginzburg-Landau type of analysis [6] would give a general law of the form $T_N(H) \approx T_N(0) - \beta H^2$ which is well obeyed by the results in figure 9.

3.2.4. Magnetisation in the basal plane (along a, b). Figure 10 shows the magnetisations measured along the a and b axes as functions of x for a high field ($H = 50$ kG) applied along a or b . First, one observes systematically that $M^b > M^a$, which seems to show that there is an anisotropy within the basal plane. Second, M increases continuously with

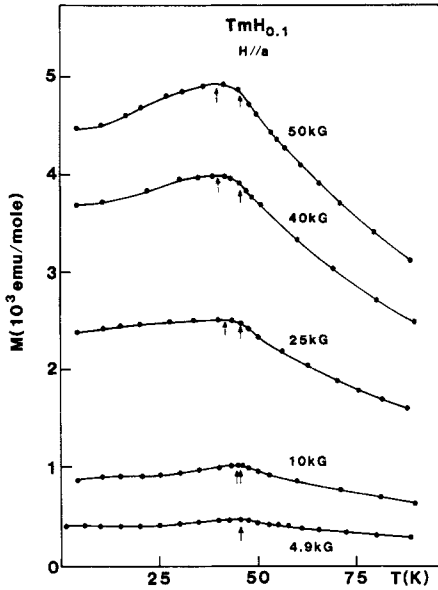


Figure 11. Temperature variation in the magnetisation M for $\text{TmH}_{0.1}$ in applied fields parallel to the a axis.

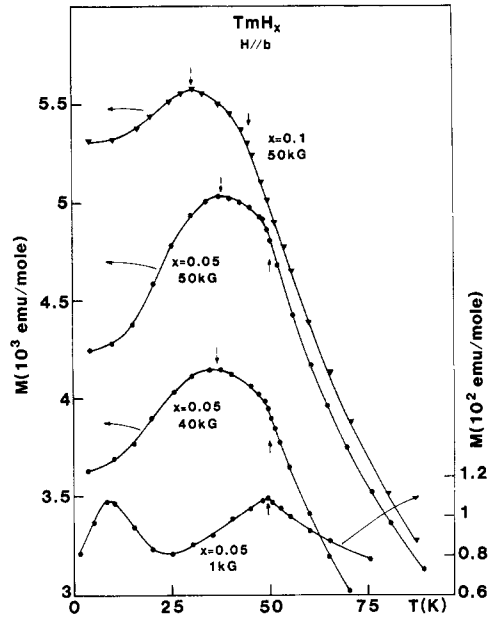


Figure 12. Temperature variation in the magnetisation M for TmH_x (with $x = 0.05$ and 0.1) in applied fields parallel to the b axis.

increasing x , i.e. the hydrogen in solution tends to reduce the anisotropy term which favours the c axis, a result which is in qualitative agreement with the fact that the magnetisation $M^{z,c}$ along the c axis decreases with increasing x (figure 6). One wonders, whether this diminishing anisotropy with increasing x is related to the same phenomenon which led to a diminishing energy gap in the spin-wave spectrum of TmH_x crystals as observed in resistivity measurements [14], namely to the fact that hydrogen in solution expands the Tm lattice, anisotropically pushing its originally contracted c/a ratio ($c/a = 1.57$) closer to the ideal value of 1.63.

Figures 11 and 12 give the variations in $M^a(T)$ and $M^b(T)$ for different fields H . Their respective behaviours are somewhat surprising. If one considers first the case $H \parallel a$ (figure 11), one observes (here, for $x = 0.1$) a well defined maximum at T_N (for AF ordering along the c axis) for $H = 5$ kG and $H = 10$ kG, in agreement with equation (4) but, for higher fields ($H \geq 25$ kG), there is a small decrease in the maximum temperature, which is not obvious. At the same time, there continues to be a small anomaly for the true T_N , i.e. a change in curvature indicated by the full arrow (while the maximum is indicated by a broken arrow); dM/dT does not change sign at T_N but decreases slightly.

This new situation is much more visible in figure 12 for $H \parallel b$; there is a well defined maximum at T_N for $x = 0.05$ and $H = 1$ kG but, for $H = 40$ – 50 kG, there is only a curvature anomaly at T_N , while the maximum occurs at a much lower T . Such a situation was observed for ErH_x [12] where the basal plane magnetisation showed two anomalies: a curvature anomaly at T_N and a maximum at T_H corresponding to the true AF basal plane transition, which *a priori* does not exist in pure Tm. One can show, following the lines of the Ginzburg–Landau model [6] that T_H exists only if $K' > 0$. For pure Tm, one has *a priori* $K' < 0$, i.e. no basal plane antiferromagnetism. However, one may wonder whether the hydrogen does not modify this situation somewhat, especially in high fields.

The results in figure 11 suggest that $K' = K'(x, H)$, i.e. K' might change sign with H for finite x -values.

4. Conclusions

All the magnetisation data taken on α -TmH_x along the c axis and in the basal plane tend to show that hydrogen has three main effects:

- (i) a decrease in the AF and ferrimagnetic transition temperatures (along the c axis) due to modifications of the electronic structure;
- (ii) a hardening of the ferrimagnetic and ferromagnetic $M(H)$ relation along the c axis due to an increase of the coercivity field or pinning of the domain walls;
- (iii) a decrease in the anisotropy between the c axis and the basal plane, which favours the basal plane magnetisation and perhaps even the occurrence of basal plane AF ordering.

References

- [1] Coqblin B 1977 *Electronic Structure of Rare Earth Metals and Alloys* (New York: Academic)
- [2] Koehler W C, Cable J W, Wollan E O and Wilkinson M K 1962 *Phys. Rev.* **126** 162
- [3] Brun T O and Lander G H 1969 *Phys. Rev. Lett.* **23** 1295
- [4] Brun T O, Sinha S K, Wakabayashi N, Lander G H, Edwards L R and Spedding F H 1970 *Phys. Rev. B* **1** 1251
- [5] Richards D B and Legvold S 1969 *Phys. Rev.* **186** 508
- [6] Burger J P, Vajda P, Daou J N and Chouteau G 1987 *J. Magn. Magn. Mater.* **67** 343
- [7] Daou J N, Vajda P, Lucasson A and Lucasson P 1980 *Solid State Commun.* **34** 959; **35** 809; 1981 *J. Phys. C: Solid State Phys.* **14** 129
- [8] Daou J N, Radhakrishna P, Tur R and Vajda P 1981 *J. Phys. F: Met. Phys.* **11** L263
- [9] Ito T, Legvold S and Beaudry B J 1983 *Phys. Rev. B* **30** 240
- [10] Daou J N, Radhakrishna P, Vajda P and Allain Y 1983 *J. Phys. F: Met. Phys.* **13** 1093
- [11] Daou J N, Vajda P, Hilscher G and Pillmayr N 1988 *J. Physique* **49** C8 357
- [12] Burger J P, Vajda P, Daou J N and Chouteau G 1986 *J. Phys. F: Met. Phys.* **16** 1275
- [13] Vajda P, Daou J N, Burger J P, Schmitzer C and Hilscher G 1987 *J. Phys. F: Met. Phys.* **17** 2097
- [14] Vajda P, Daou J N, Burger J P, Hilscher G and Pillmayr N 1989 *J. Phys.: Condens. Matter* **1** 4099
- [15] Misemer D K and Harmon B W 1982 *Phys. Rev. B* **26** 5634
- [16] Rhyne J J and Legvold S 1965 *Phys. Rev.* **140** A2143
- [17] Miwa H and Yosida K 1961 *Prog. Theor. Phys.* **26** 693